



Optics Letters

Sub-second quantum cascade laser based infrared spectroscopic ellipsometry

ALEXANDER EBNER,¹  ROBERT ZIMMERLEITER,¹ CHRISTOPH COBET,² KURT HINGERL,³
MARKUS BRANDSTETTER,^{1,*}  AND JAKOB KILGUS¹

¹RECENDT—Research Center for Non-Destructive Testing GmbH, Science Park 2, Altenberger Str. 69, 4040 Linz, Austria

²Linz School of Education, Johannes Kepler Universität, Altenberger Str. 69, 4040, Linz, Austria

³Center for Surface and Nanoanalytics, Johannes Kepler Universität, Altenberger Str. 69, 4040, Linz, Austria

*Corresponding author: markus.brandstetter@recendt.at

Received 1 May 2019; revised 5 June 2019; accepted 5 June 2019; posted 5 June 2019 (Doc. ID 366212); published 3 July 2019

Laser-based infrared spectroscopic ellipsometry (SE) is demonstrated for the first time, to the best of our knowledge, by applying a tunable quantum cascade laser (QCL) as a mid-infrared light source. The fast tunability of the employed QCL, combined with phase-modulated polarization, enabled the acquisition of broadband (900–1204 cm⁻¹), high-resolution (1 cm⁻¹) ellipsometry spectra in less than 1 second. A comparison to a conventional Fourier-transform spectrometer-based IR ellipsometer resulted in an improved signal-to-noise ratio (SNR) by a factor of at least 290. The ellipsometry setup was finally applied for the real-time monitoring of molecular reorientation during the stretching process of an anisotropic polypropylene film, thereby illustrating the advantage of sub-second time resolution. The developed method exceeds existing instrumentation by its fast acquisition and high SNR, which could open up a set of new applications of SE such as ellipsometric inline process monitoring and quality control. © 2019 Optical Society of America

<https://doi.org/10.1364/OL.44.003426>

Provided under the terms of the [OSA Open Access Publishing Agreement](#)

The already well-established measurement technique ellipsometry gained an increasingly important role in various scientific and industrial disciplines resulting in numerous technological and biomedical applications [1]. Ellipsometry is based on the determination of a polarization change due to light-matter interaction at a sample [2]. This change in polarization can arise from various processes at the surface or inside the bulk leading to a wide range of measurable sample parameters. As the method relies on the measurement of intensity ratios of polarization components, including their phase difference, the complex refractive index can be obtained directly without any reference measurements or performing a Kramers–Kronig analysis. Thereby, unique information about the sample such as chemical composition, as well as dielectric and geometric properties, can be obtained simultaneously. Additionally, ellipsometry offers extraordinary sensitivity enabling sub-monolayer resolution, e.g., in epitaxial thin film growth [3,4].

By means of spectroscopic ellipsometry (SE), wavelength-dependent sample properties are probed. The spectral regions covered by SE span the ultra-violet (UV), visible (VIS) and infrared (IR) spectral range. Whereas the UV and VIS regions are sensitive to electronic states and excitons, in the IR molecular vibrations, free-carrier and phonon absorptions are observed. In contrast to free-carrier absorptions probed in the terahertz range [5], fundamental vibration modes occur in the fingerprint region, which is part of the mid-infrared (MIR) spectral range. Therefore, SE in the MIR enables the determination of both chemical composition and, in the case of anisotropy, spatial orientation of the investigated structure. However, until recently, optical methods in the MIR range had to rely on thermal light sources. Such sources feature low brilliance—defined as photon flux per solid angle and bandwidth—leading to long integration times and to a significant loss of intensity after large path lengths or penetration depths.

The advent of quantum cascade lasers (QCLs) eventually brought a unique, spectrally tunable, and high-brilliance MIR laser source. Thus, the advantages of lasers could be combined with the ability of broadband emission known from thermal light sources. QCLs are monochromatic sources, but offer a spectral tuning range up to several 100 cm⁻¹ when realized in external cavity configuration (EC-QCL) [6]. Hence, spectroscopic measurements without the need of any monochromator or interferometer became feasible [7]. In comparison to thermal MIR light sources, QCLs offer at least 10⁴ times higher brilliance. The provided improvements in signal-to-noise ratio (SNR) and sensitivity enable new applications such as transmission measurements of liquid solutions beyond the limits of conventional systems if the characteristic properties of EC-QCLs are considered [8,9]. Furthermore, the fast tunability of several 1000 cm⁻¹/s leads to a major reduction of the acquisition time per spectrum.

The advantage of using a high-brilliance QCL for vibrational circular dichroism measurements has already been shown by Lüdeke *et al.* [10]. Thereby, the efficiency of QCLs applied to a polarization-modulating technique was demonstrated in spectral regions that are difficult to study due to significant water absorption. However, the potential high time resolution

could not be exploited, as the application of a chopper drastically reduces the available sampling rate. Compared to dichroism measurements, ellipsometry turns out to be a more powerful method, as both phase shift and amplitude ratio—expressed by the ellipsometric parameters Δ and Ψ —are recorded simultaneously. Therefore, SE additionally covers dichroism information and is not limited to anisotropic samples. The first application of ellipsometry using a QCL was presented by mapping structured surfaces and molecular interactions in organic thin films at only two discrete wavelengths [11]. The presented results demonstrate a promising outlook in terms of hyperspectral sample mapping ellipsometry. However, the potential of realizable diffraction-limited spot sizes offered by QCLs was not exploited, as only a spatial resolution in the millimeter range was achieved.

In our contribution, we present, to the best of our knowledge, the first laser based SE measurements by recording continuous spectra (900–1204 cm^{-1}) with 1 cm^{-1} resolution in sub-second acquisition times (887 ms per Δ , Ψ -spectrum). In order to demonstrate the accuracy of the developed system, anisotropic polypropylene (PP) films of 6 μm thickness have been measured in transmission at normal incidence and were compared with reference measurements done with a commercially available Fourier-transform infrared (FTIR) spectroscopy-based rotating compensator ellipsometer. Furthermore, the enhanced noise performance of the presented setup compared to the conventional ellipsometer is shown. Finally, the spatial reorientation of molecules within a PP film due to an applied tensile force has been observed with the sequential recording of multiple ellipsometry spectra. This realization of laser based SE measurements opens up new paths and opportunities for future research in the MIR spectral range.

The configuration of the developed QCL ellipsometer is illustrated in Fig. 1. The applied EC-QCL (DRS Daylight Solutions Hedgehog) is tunable from 900 cm^{-1} to 1204 cm^{-1} (1000 cm^{-1}/s) while emitting a laser beam with a waist of about 2.5 mm in the TEM_{00} spatial mode (linearly polarized >100:1). In the presented setup the laser was driven in continuous wave mode leading to an extremely narrow spectral linewidth of just $3.3 \times 10^{-3} \text{ cm}^{-1}$ and a maximum emission power of 110 mW according to the manufacturer. Combined with high wavelength repeatability ($\leq 0.1 \text{ cm}^{-1}$), accuracy

($\leq 0.5 \text{ cm}^{-1}$) and precision ($\leq 0.2 \text{ cm}^{-1}$), measurements with a spectral resolution below 1 cm^{-1} were feasible. For polarization modulation a ZnSe photo-elastic modulator (PEM) operating at 37 kHz (Hinds Instruments PEM-90) was used. The signal was detected with a thermoelectrically cooled mercury cadmium telluride (MCT) detector (VIGO System PCI-4TE-12). In order to split the detected signal into an AC as well as a DC part, a signal extraction unit consisting of a high-pass filter (10 kHz) and a low-pass filter (10 Hz or 2 kHz depending on the acquisition speed) was implemented. For further signal processing, a digital lock-in amplifier (LIA) (Anfatec Instruments eLockIn 204) offering multiple signal outputs was used. Finally, the desired signals were recorded by means of a 12 bit high-speed oscilloscope (Teledyne LeCroy HDO6104A).

As indicated in Fig. 1, the vertically polarized QCL radiation was passed through a slightly tilted KBr window to prevent back reflections into the laser. In order to avoid interference effects at the modulation frequency, the laser beam diameter was reduced to about 0.6 mm by an aperture before the beam passed the 15° tilted PEM. Additionally, to sub-millimeter spot sizes, this configuration allows splitting the first transmitted beam from the ones experiencing multiple reflections in the optical element of the PEM. The latter were then blocked by a razor blade placed directly behind the PEM. After passing the sample, the transmitted radiation was analyzed by four successively arranged wire grid polarizers before a ZnSe lens focused the beam on the detector chip. The detected intensity I_{det} was calculated by means of Jones matrices of the respective optical elements. In the given configuration with a PEM optical axis and analyzer, each rotated 45° with respect to the initial polarization, this leads to

$$I_{\text{det}} \sim I_0 + I_0 J_0(\delta_0) \cos(2\Psi) \rightarrow I_{\text{DC}} \\ + 2I_0 J_1(\delta_0) \sin(2\Psi) \sin(\Delta) \sin(\omega_M t) \rightarrow I_\omega \quad (1) \\ + 2I_0 J_2(\delta_0) \cos(2\Psi) \cos(2\omega_M t) \rightarrow I_{2\omega},$$

after Jacobi–Anger expansion [12]. Here I_0 denotes the intensity provided by the QCL, while δ_0 and ω_M refer to the modulation amplitude and modulator circular frequency, respectively. The Bessel functions arising due to the expansion are given by J_0, J_1 , and J_2 . As indicated in Eq. (1), the detected intensity can be split into three terms with different temporal dependences. Whereas the temporally constant intensity is directly extracted by the low-pass filter of the signal extraction unit, the intensity amplitudes I_ω and $I_{2\omega}$ of the temporally varying parts are processed by lock-in amplification. Finally, the ellipsometric parameters Δ and Ψ arise from the solution of the resulting system of three non-linear equations and are given by

$$\Psi = \frac{1}{2} \cos^{-1} \left(\frac{I_{2\omega}}{2I_{\text{DC}} J_2(\delta_0) - I_{2\omega} J_0(\delta_0)} \right), \quad (2)$$

$$\Delta = \sin^{-1} \left(\frac{1}{\sin(2\Psi) 2I_{\text{DC}} J_1(\delta_0) - I_{2\omega} J_0(\delta_0) \frac{J_1(\delta_0)}{J_2(\delta_0)}} \right). \quad (3)$$

In contrast to previous work, Eqs. (2) and (3) are not restricted to certain modulation amplitudes. If the peak-to-peak voltage provided by the PEM controller is held constant, δ_0 is wavelength-dependent and can be determined as a parameter in a fitting procedure. For this purpose, the theoretically derived

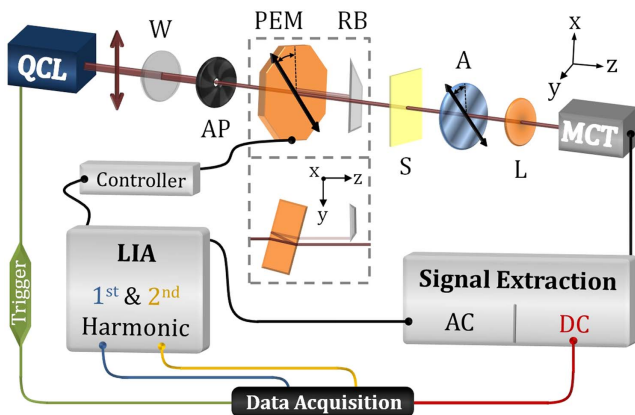


Fig. 1. (a) Experimental setup. QCL, quantum cascade laser; W, KBr window; AP, aperture; PEM, photo-elastic modulator; RB, razor blade; S, sample; A, analyzer unit; L, lens; MCT, mercury cadmium telluride detector.

and not expanded intensity I_{det} was fitted to raw intensity signals recorded for each wavelength without using the signal extraction unit and the LIA. The wavelength-dependent modulation amplitude calculated for the whole spectrum stays valid unless the applied voltage or PEM alignment is changed.

To tune the emitted wavelength of the QCL, two reasonable tuning modes were available. On the one hand, stepwise tuning with acquisition times of 58 s for a full spectrum—referred to as the step and measure mode—turned out to be the most precise choice, as the dwell time of 180 ms per 1 cm^{-1} step allowed averaging a large number of signals at each step. On the other hand, the continuous tuning in the sweep mode enabled the fast acquisition of full spectra in 887 ms. In the latter case, the recorded measurement points of a single spectrum were averaged to a still very high spectral resolution of 1 cm^{-1} . Additionally, a potential spectral shift due to nonlinear wavelength tuning was compensated for by correlation optimized warping [13].

Figure 2 shows ellipsometry spectra of anisotropic $6 \mu\text{m}$ PP films recorded in normal incidence transmission measurements. All of them display prominent bands at 1168 , 998 , and 973 cm^{-1} , as well as very weak bands at 1103 and 1045 cm^{-1} , with their origin already investigated elsewhere [14]. The active groups responsible for the respective prominent features are indicated in the graph. As features observed in normal incidence ellipsometry spectra are directly related to sample anisotropy (with respect to the optical axis of the PEM), a non-homogeneously distributed orientation of polymer chains was determined. To demonstrate the accuracy of the QCL ellipsometer, the acquired spectra were compared to spectra recorded with a commercially available Woollam IR-VASE rotating compensator ellipsometer based on a thermal light source and FTIR spectroscopy. All measurements were performed with 1 cm^{-1} spectral resolution and smoothed with a 3 cm^{-1} moving average algorithm. While the displayed QCL spectra were acquired in a single measurement lasting 58 s (step

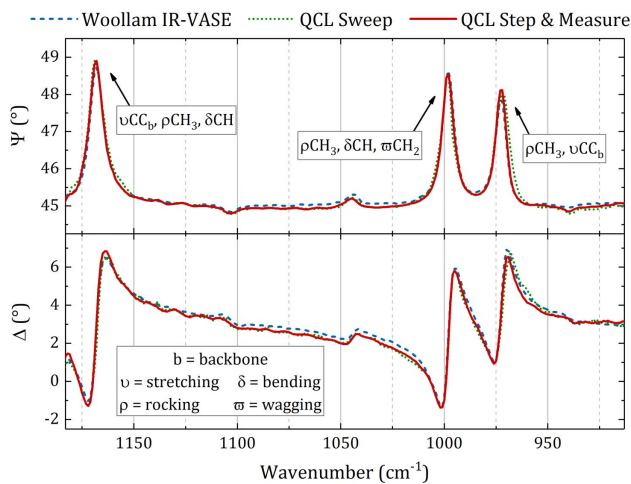


Fig. 2. Ellipsometry spectra of anisotropic $6 \mu\text{m}$ PP films recorded in normal incidence transmission measurements with a Woollam IR-VASE (blue) and the presented QCL ellipsometer in sweep (green) and step and measure modes (red). The active groups responsible for the prominent observed features are indicated. QCL spectra were acquired in single measurements; Woollam IR-VASE spectra result from averaging 200 spectra.

and measure), and 887 ms (sweep), the Woollam spectra result from averaging 200 broadband spectra ($292\text{--}6410 \text{ cm}^{-1}$) acquired in 323 s each.

QCL ellipsometry enables data acquisition in a fraction of the time necessary with conventional systems without a loss in SNR. In fact, the SNR can even be improved significantly, as indicated by the different axis labels and the standard deviation (SD) given in Fig. 3. In order to highlight the exceptional noise characteristics of the QCL-based system, normalized ellipsometry spectra are illustrated. For this purpose, the ratios of two unsmoothed spectra were calculated for the measurements with the Woollam IR-VASE, as well as each of the two QCL ellipsometry measurement methods. Compared to Woollam's IR-VASE, the QCL ellipsometer showed a factor of 15 improved noise performance at an approximately 360-fold reduced acquisition time in the sweep mode. Thus, this would lead to a SNR enhancement by a factor of 290 ($15 \times \sqrt{360}$).

The real-time capability of QCL ellipsometry was demonstrated by the observation of molecular reorientation within a $6 \mu\text{m}$ PP film. As stated above, the polymer chains of the film exhibited non-homogeneously distributed orientation prior to stretching. Therefore, the investigated film was fixed in a tensile stage with the predominant direction of the molecular chains orientated perpendicular to the applied force. Increasing the tensile force reorients PP chains parallel to the stretching direction and, thus, leads to a reduction of anisotropy as active groups start to reach a homogeneous orientation. Further stretching of the PP film again introduces anisotropy as the polymer chains attain a predominant orientation parallel to the applied force and perpendicular to the initial arrangement.

The stretching experiment took 850 s until the breaking point of the film, limited only by the slow movement of the jaws (1 mm/min). The process was continuously monitored by recording 678 ellipsometry spectra in the sweep mode. For better illustration, Fig. 4 only shows every 30th recorded Ψ -spectrum. Due to the high acquisition speed, an increase of the tensile force during the recording of a single Δ , Ψ -spectrum is negligible. As indicated in the graph, the blue spectra recorded at the beginning of the experiment imply predominant orientation of the polymer chains perpendicular to the applied

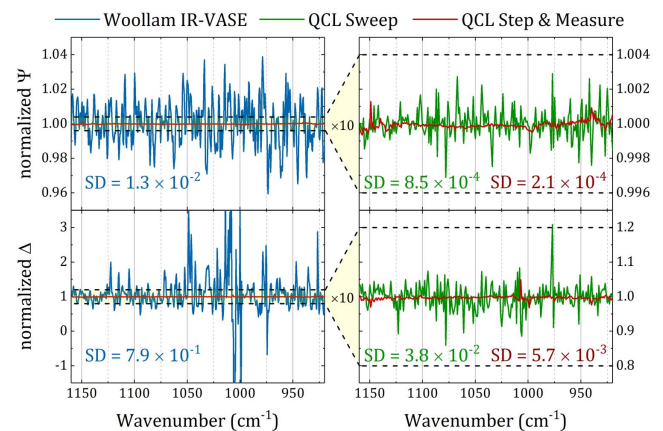


Fig. 3. Normalized ellipsometry spectra for noise illustration recorded with a Woollam IR-VASE (blue) and the presented QCL ellipsometer in sweep (green) and step and measure modes (red). The SD of each spectrum is given below the respective graph.

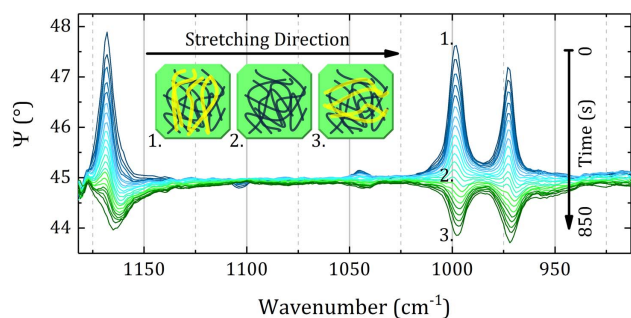


Fig. 4. Ellipsometry spectra of an anisotropic 6 μm PP film recorded in a normal incidence transmission measurement. During data acquisition, the film was stretched by an applied tensile force. The spectra were recorded in the sweep mode in less than 1 s per spectrum. The predominant orientation of polymer chains in advancing levels of distortion is indicated.

force, whereas the green spectra indicate a preferred orientation along the stretching direction.

In summary, a new level of performance for SE in the MIR range could be achieved by exploiting a QCL as a broadband and high-brilliance light source. The outstanding advantages of QCL ellipsometry in terms of acquisition speed and noise performance were demonstrated by comparing the presented system to a commercially available rotating compensator ellipsometer based on FTIR spectrometry and a thermal light source. The possibility to acquire high-quality Δ , Ψ -spectra in less than 1 s was utilized for monitoring the stretching process of a PP film. Thereby, SE in the MIR range allowed the direct observation of the reorientation of molecular functional groups within the film. The implementation of IR SE in time-critical monitoring applications, in which the signal is already strongly attenuated by the sample, can now be realized with the developed approach. Furthermore, the provided enhancement in SNR by the high brilliance of MIR broadband lasers can significantly reduce detection limits [15].

As phase-modulated ellipsometry measures ratios of the polarization components, including their phase information, no reference measurement for normalization purpose is necessary. Therefore, SE is hardly affected by instabilities of the light source, atmospheric absorption and ambient unpolarized stray light. This self-calibration scheme, similar to balanced detection, illustrates a great benefit of ellipsometry, e.g., for long-term measurements in quality control or inline process monitoring. Especially in biomedicine broadband, high-brilliance MIR lasers already brought decisive advantages, e.g., for fast blood analysis or diffraction-limited imaging of blood cells [16,17]. Adding the benefits of ellipsometry to this kind of measurements would enable monitoring the MIR complex refractive index of strongly absorbing liquids (similar to [18]) or generating high-resolution images of biomolecular surface structures with enhanced sensitivity not yet accessible.

With the presented approach, the powerful technique SE is combined with the unique features of QCLs—such as high brilliance and small beam widths at broadband spectral coverage—enabling new opportunities for future research in the MIR spectral range.

Funding. European Regional Development Fund (ERDF) (IWB2020); Province of Upper Austria (Innovative Upper Austria 2020).

Acknowledgment. The authors acknowledge financial support by the strategic economic-research program “Innovative Upper Austria 2020” of the province of Upper Austria and the project “Multimodal and in-situ characterization of inhomogeneous materials” (MiCi) by the federal government of Upper Austria and the European Regional Development Fund (ERDF) in the framework of the EU-program IWB2020.

REFERENCES

1. M. Losurdo, M. Bergmair, G. Bruno, D. Cattelan, C. Cobet, A. De Martino, K. Fleischer, Z. Dohcevic-Mitrovic, N. Esser, M. Galliet, P. Gajic, D. Hemzal, K. Hingerl, J. Humlicek, R. Ossikovski, Z. V. Popovic, and O. Saxl, *J. Nanopart. Res.* **11**, 1521 (2009).
2. H. Fujiwara, *Spectroscopic Ellipsometry: Principles and Applications* (Wiley, 2007).
3. G. A. Bootsma and F. Meyer, *Surf. Sci.* **14**, 52 (1969).
4. E. H. Korte and A. Röseler, *Analyst* **123**, 647 (1998).
5. T. Hofmann, C. M. Herzinger, A. Boosalis, T. E. Tiwald, J. A. Woollam, and M. Schubert, *Rev. Sci. Instrum.* **81**, 023101 (2010).
6. A. Lambrecht, M. Pfeifer, W. Konz, J. Herbst, and F. Axtmann, *Analyst* **139**, 2070 (2014).
7. D. Caffey, M. B. Radunsky, V. Cook, M. Weida, P. R. Buerki, S. Crivello, and T. Day, in *Novel In-Plane Semiconductor Lasers X* (2011), p. 79531K.
8. M. Brandstetter, T. Sumalowitzsch, A. Genner, A. E. Posch, C. Herwig, A. Drolz, V. Fuhrmann, T. Perkmann, and B. Lendl, *Analyst* **138**, 4022 (2013).
9. M. Brandstetter, C. Koch, A. Genner, and B. Lendl, *Quantum Sensing and Nanophotonic Devices XI* (2014), p. 89931U.
10. S. Lüdeke, M. Pfeifer, and P. Fischer, *J. Am. Chem. Soc.* **133**, 5704 (2011).
11. A. Furchner, C. Kratz, D. Gkogkou, H. Ketelsen, and K. Hinrichs, *Appl. Surf. Sci.* **421**, 440 (2017).
12. O. Acher, E. Bigan, and B. Drévilion, *Rev. Sci. Instrum.* **60**, 65 (1989).
13. G. Tomasi, F. Van Den Berg, and C. Andersson, *J. Chemom.* **18**, 231 (2004).
14. J. Karger-Kocsis, *Polypropylene: An A-Z Reference* (Kluwer, 1999).
15. C. Gasser, J. Kilgus, M. Harasek, B. Lendl, and M. Brandstetter, *Opt. Express* **26**, 12169 (2018).
16. M. Brandstetter, L. Volgger, A. Genner, C. Jungbauer, and B. Lendl, *Appl. Phys. B* **110**, 233 (2013).
17. J. Kilgus, G. Langer, K. Duswald, R. Zimmerleiter, I. Zorin, T. Berer, and M. Brandstetter, *Opt. Express* **26**, 30644 (2018).
18. D. J. Rowe, D. Smith, and J. S. Wilkinson, *Sci. Rep.* **7**, 7356 (2017).